

Supporting Information

All-Conjugated Donor-Acceptor Block Copolymers featuring a Pentafulvenyl-Polyisocyanide-Acceptor

Sandra Schraff, Sudeshna Maity, Laura Schleeper, Yifan Dong, Sebastian Lucas,

Artem A. Bakulin, Elizabeth von Hauff, Frank Pammer

Contents

1. Materials and Instrumentation	2
2. Synthetic Procedures	3
2.1. Synthesis of Poly(3DT- <i>block</i> -IC2) (BP11, BP21, BP31).....	3
2.2. Synthesis of Poly(TzTHX- <i>block</i> -IC2) (BP4).....	3
Table S1. Properties of new block-copolymers, and reference data for corresponding homo polymers.....	4
Table S2. Block copolymer composition determined by EDX-spectroscopy, end-group analysis via NMR, and from GPC-data.....	4
3. Supplementary Analytical Data.....	5
Figure S1. GPC-Elution traces of a) P(3DT- <i>b</i> -IC2) (feed 1:1) and b) P(3DT- <i>b</i> -IC2) (feed 2:1 and 3:1), and GPC traces of the corresponding P3DT-homo blocks. Elution at 1mL/min, 35°C in THF.	5
Figure S2. GPC-Elution traces of BP4.	5
Figure S3. ¹ H NMR spectrum of P(3DT- <i>b</i> -IC2) (feed 1:1).....	5
Figure S4. ¹ H NMR spectrum of P(TzTHX- <i>b</i> -IC2) (BP4).....	6
Figure S5. ¹ H NMR spectra of anisyl-capped P3DT.	6
Figure S6. TGA thermograms of BP11, BP21, BP31 (A) and BP4 (B).	7
Figure S7. DSC thermograms of homo- and block-copolymers.	7
Figure S8. Fluorescence spectra of BCPs in solution vs. in the solid state. A) BP31 and BP21, B) BP4. All solution spectra recorded in DCM.	8
Figure S9. Aggregation of a P3DT in hot hexane monitored by UV-vis absorption	8
Figure S10. BP4 in n-heptane solution monitored by UV-vis absorption and fluorescence spectroscopy.	8
Figure S11. Temperature dependent UV-vis-data of PTzTHX in hexane solution. A) Absorption spectra. B) Fluorescence spectra. C) Comparison of fluorescence of BP4 and PTzTHX in solution.	9
Figure S12. A) Absorption spectra BP4 in DCM solution and of thin films, B) and emission spectrum recorded in DCM solution.....	9
Figure S13. UV-vis spectra of BPCs reproduced by overlay of homo polymer spectra.	9
Figure S14. SAXS and WAXS refractograms of aggregated BP11 (A) and BP21 (B)...	10
Figure S15. SAXS (black) and WAXS (red/gray) refractograms of BP31 and a reference sample of P3DT.	10

4. Electron Microscopy Data	11
Figure S16. Scanning electron micrographs of aggregated BP11.....	11
Figure S17. Scanning Electron Micrographs of aggregated BP21.	11
Figure S18. Scanning Electron Micrographs of aggregated BP31 after fast cooling. .	12
Figure S19. Transmission Electron Micrographs of aggregated BP31 after fast cooling.	12
Figure S20. Scanning Electron Micrographs of aggregated BP31 after slow cooling.	13
5. Electrical characterization and devices	14
5.1. Test in block-copolymer solar cells.....	14
Figure S21. Device architecture used for block-copolymer solar cell.....	14
Figure S22. Current-Voltage curve for OSC-devices from BP11, BP21, and BP31.....	14
5.2. Electrical characterization of PIC1 – PIC3	15
Figure S23. Device architectures used for mobility measurements.....	15
Figure S24. Current density versus Voltage (JV) curves of three exemplary single carrier devices, the inset image shows corresponding log J versus log V fitted curve used for the calculation of mobility (A) Hole-only diode behavior and (B) Electron-only diode behavior.....	16
Table S4. Summary of mobility measurements for PIC1, PIC2, and PIC3.....	16
6. References	17

Experimental Section and Supplementary Analytical Data

1. Materials and Instrumentation

All reactions and manipulations of sensitive compounds were carried out under an atmosphere of pre-purified argon using either Schlenk techniques or an inert-atmosphere glovebox (MBraun Labmaster, Sylatech GB 1500-E). Toluene, Et₂O, THF, DMF and dichloromethane were purified using a solvent purification system (MBraun; alumina / copper columns for hydrocarbon solvents). Hexane and benzene were dried by distillation from CaH₂ under argon atmosphere prior to use. 5-(4-isocyanobenzylidene)-1,2,3,4-phenylcyclopentadiene,¹ and 2-bromo-3-dodecyl-5-iodothiophene,² 5-bromo-2-chloro-4-(trihexylsilyloxymethyl)-thiazole,³ and Ni(*o*-anisyl)(dppe)Br⁴ were prepared according to published procedures. PFN-P1 (Poly[(9,9-bis(3'-(N,N-dimethylamino)propyl)-2,7-fluorene)-alt-2,7-(9,9-dioctylfluorene)]) were purchased from 1-MATERIAL and Chlorobenzene (Anhydrous, 99.8%) was purchased from Sigma-Aldrich. Other reagents were commercially available (Aldrich, Acros, Alfa Aesar) and were either used as obtained or purified by standard procedures.⁵ ¹H-, ¹³C- and ³¹P-NMR spectra were recorded at 293 K on a Bruker Avance DRX 400 (400 MHz) spectrometer or a Bruker Avance 500 AMX (500 MHz). Solution ¹H and ¹³C NMR spectra were referenced internally to the solvent residual signals.⁶ UV-visible absorption spectra and photoluminescence spectra were acquired on a Perkin Elmer Lambda 19 UV-vis/NIR spectrometer and a Perkin Elmer LS 55 fluorescence spectrometer, respectively.

Thermal gravimetry measurements were carried out on a TGA/SDTA 851e by Mettler Toledo, with an Al₂O₃ 70µL sample holder 25-800°C, 10°C/min 50ml/min N₂, Software STARe Version 9.30.

Powder X-ray diffraction: Wide Angle X-Rays scattering: PXRD-measurements were taken on a PANalytical X'Pert MPD Pro using copper radiation (Kα1 = 1.5405980 Å), equipped with an X'Celerator-detector.

Electron Microscopy: Scanning Electron Microscopy (SEM), Transmission Electron Microscopy (TEM) and Energy-dispersive X-ray spectroscopy (EDX) were performed with support from Prof. Dr. Paul Walther⁷ and coworkers at the electron microscopy department of the University of Ulm. SEM micrographs were recorded either on a Helios Nanolab 600 (Thermo Fisher Scientific) or on an Hitachi S-5200 Fe-SEM. Images were recorded in analysis mode of the secondary electron signal. TEM was measured on a Jeol 1400 TEM (Jeol, Tokyo, Japan) with voltage of 120 kV. Images were recorded with a Veleta CCD Kamera (Olympus, Münster, Germany) and digitized with the iTEM Software 5.2 (Olympus). EDX spectroscopy was performed on a Quanta 3D FEG (Thermo Fisher Scientific) equipped with

an Apollo XV SDD EDX Detector (EDAX-AMETK). The data was analyzed and processed with the Genesis 6.5 Software-Package (EDAX AMETEK). SEM- and EDX-samples were drop-cast on glass-slides (Menzelgäser) and metallized with 150 Hz of platinum or carbon before measurements. TEM samples were drop-cast on copper grids (Plano GmbH) and were measured without prior treatment.

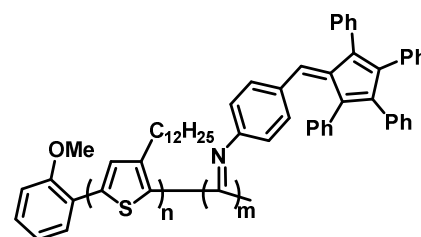
Transient Absorption Spectroscopy (TAS). For TAS, a 1 kHz Ti:sapphire regenerative amplifier (Spectra-Physics Solstice, Newport Corporation) provided seed pulses (800 nm, ~ 100 fs) for the pump and probe. The pump was generated by an optical parametric amplifier (TOPAS, Light Conversion) coupled to a frequency mixer (NIRUVis, Light Conversion), whereas the broad-band NIR probe (~ 850 – 1350 nm) was generated in an yttrium aluminum garnet crystal inside the commercially available TAS setup (HELIOS, Ultrafast Systems). The pump and probe were focused onto a 0.5 mm 2 spot on the sample, which was placed in an N₂-purged cuvette for measurements. The pump was modulated at 500 Hz, and the delay between the pump and probe was controlled with a mechanical stage in the probe beam path. All analyses were conducted in MATLAB and Origin. The measurements were performed by time-correlated single photon counting (TCSPC). Kinetics were studied at 660 nm after an excitation at 467 nm. The kinetics of ultrafast TA measurements (Figure D-F) are performed with a 500 nm pump beam having an intensity of 20 μJ/cm² and near 1200 nm infrared probe beam.

2. Synthetic Procedures

2.1. Synthesis of Poly(3DT-*block*-IC2) (BP11, BP21, BP31)

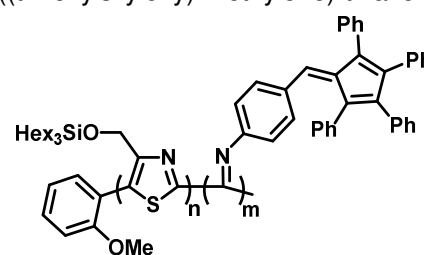
BP11: Inside a glovebox under argon atmosphere 2-brom-5-iodo-3-dodecylthiophen (**1**, 72.0 mg, 157 μmol, 1.0 Eq.) was dissolved in 1.3 mL of dry THF and a solution of ⁱPrMgCl·Et₂O (27.0 mg, 153 μmol, 1.0 Eq.) in 1.3 mL dry THF was added. The reaction mixture was stirred for 30 min at ambient temperature, and subsequently 0.76 mL (2 mol-%) of a solution of Ni(*o*-anisyl)(dppe)Br (4.13 mmol/L in THF) were quickly injected. The reaction mixture was stirred for another 2 h, after which a sample was taken for analyses by GPC, and a solution of isocyanide **3 b** (76.0 mg, 157 mmol, 1.0 Eq.) in 1.3 mL of dry THF was added. Subsequently, the reaction mixture was quenched by pouring it into methanol, and the precipitate was washed on a glass fiber filter with MeOH, Acetone, and n-hexane, followed by extraction with dichloromethane. The DCM-fraction was concentrated diluted with benzene, and freeze-dried to furnish 72.1 mg of **BP11**.

BP21/BP31: Thiophene **1** (103 mg, 225 μmol) was metalated and polymerized with 2 mol-% of Ni(*o*-anisyl)(dppe)Br as described above, and a GPC-sample was taken. The reaction mixture was then divided by weight into two equal parts, and 0.50 and 0.33 equivalents of isocyanide **3** were added, respectively. The polymers were isolated by precipitation into methanol and purified by washing on a Soxhlet-apparatus with MeOH, acetone, and n-hexane, followed by extraction with Chloroform, and freeze-drying from benzene. The procedure yielded 27.5 mg of **BP21** and 26.0 mg of **BP31**.



2.2. Synthesis of Poly(TzTHX-*block*-IC2) (BP4)

Inside a glovebox under argon atmosphere a 5-Bromo-2-Chloro-4-((trihexylsilyloxy)-methylene)-thiazole (**2**, 73 mg, 143 μmol, 1.0 Eq.) was dissolved in 1.0 mL of dry THF and a solution of ⁱPrMgCl·Et₂O (25.0 mg, 143 μmol, 1.0 Eq.) in 0.8 mL THF was added, and the reaction mixture was stirred for 30 min at ambient temperature. Subsequently, 0.46 mL (2 mol-%) of a solution of Ni(*o*-anisyl)(dppe)Br (6.20 mmol/L in THF) were quickly injected, and the mixture was stirred for another 4 h. A sample of the homopolymer was then taken, a solution of the isocyanide **3** (70.0 mg, 143 μmol, 1.0 Eq.) in 1.1 mL THF was injected, and the mixture was stirred for 19 h. Subsequently, the reaction was quenched by addition of methanol, and the precipitating polymer was filtered off. The crude polymer was purified by sequential



washing with methanol and acetone on a Soxhlet apparatus, followed by extraction with *n*-hexane. The *n*-hexane-fraction was then further fractionated by preparative GPC to furnish 30 mg of the main fraction of **BP4**. Unless stated otherwise, all analytical studies have been performed with this purified fraction.

Table S1. Properties of new block-copolymers, and reference data for corresponding homo polymers.

BCP	Feed ratio n/m	GPC								NMR	
		PT / PTz-Block		Block-Copolymers						PT-block	PIC2-block
		Mn [kg/mol]	PDI	Mn [kg/mol]	PDI	n : m		n : m		Mn [kg/mol]	Mn [kg/mol]
BP11	1/1	15.7	1.05	22.9	1.06	63	15	50	59	12.5	28.5
BP21	2/1	20.8	1.02	24.5	1.03	83	8	53	42	13.5	20.3
BP31	3/1	20.8	1.02	21.4	1.03	83	1	53	8	13.0	3.9
BP4 ^[a]	1/1	33.6	1.13	38.4	1.04	85	10	89	39	35.2	18.9

Table S1 continued.

BCP	Feed ratio n/m	TGA		UV-vis Absorption				E _g ^{opt}	Emission	
		m _{res} ^[b]	T _D ^[b]	Solution		Film			Solution	Film
		%	[°C]	λ _{max} ^[c] [nm]	λ _{onset} ^[c] [nm]	λ _{max}	λ _{onset}		λ _{max} ^[c]	
BP11	1/1	28	335	380	550	605 (sh), 373	649	1.91	578	--
BP21	2/1	21	328	406	533	605, 558, 523	650	1.91	577	--
BP31	3/1	17	284	441	539	610, 561, 525	653	1.90	577	--
BP4 ^[a]	1/1	29	336	483	545	545 (sh), 502	578	2.26	545, 581	--
P3DT ^[d,f]		17	445	445	545	607, 558, 525	655	1.89	577	
PTzTHX ³		14	408	486	545	509	575	2.16	548, 590 ^[e]	588
PIC2 ⁸		43	365	368	520	381	560	2.21	--	--

[a] After purification by preparative GPC. [b] m_{res} = Residual masses at 800°C. T_D = decomposition temperature. Data for **PIC2**⁸ and **PTzTHX**³ adopted from literature, data for **P3DT** newly recorded by the authors. [c] Recorded in DCM-solution. [d] Absorption data adopted from Ref.⁹, [e] Recorded in THF³. [f] Prepared analogously to the macroinitiators for **BP11-BP31**, Mn = 24.5kg/mol, PDI = 1.10.

Table S2. Block copolymer composition determined by EDX-spectroscopy, end-group analysis via NMR, and from GPC-data.

	N [mol%] EDX	S [mol%] EDX	S/N ratio EDX	S/N ratio NMR	S/N ratio GPC
BP11	2.97 (±0.14)	1.41(±0.01)	0.5:1	0.85:1	4.2:1
BP21	2.75 (±0.48) ^[a]	5.36 (±0.24) ^[a]	2:1	1.26:1	10:1
BP31	1.70 (±0.16) ^[a]	7.70 (±0.31) ^[a]	4.5:1	6.6:1	83:1
BP4	3.19	2.71	5.7:1	2.2:2	8.5:1

[a] Average of three different measurements on aggregated material. Sampled metallized with platinum before measurement.

3. Supplementary Analytical Data

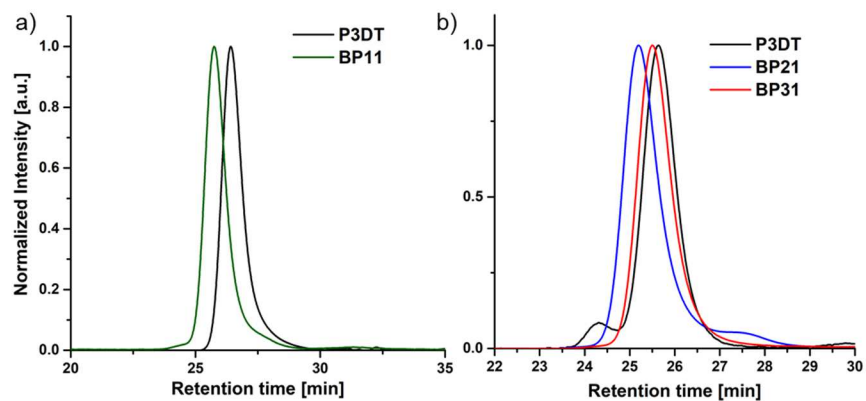


Figure S1. GPC-Elution traces of a) **P(3DT-b-IC2)** (feed 1:1) and b) **P(3DT-b-IC2)** (feed 2:1 and 3:1), and GPC traces of the corresponding **P3DT**-homo blocks. Elution at 1 mL/min, 35°C in THF.

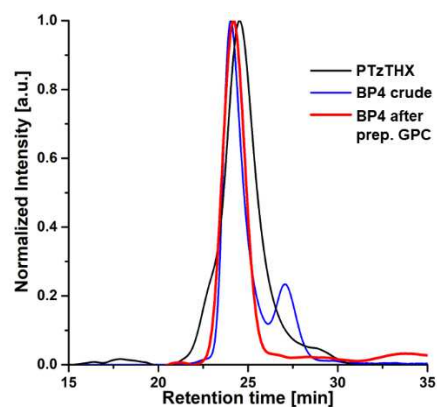


Figure S2. GPC-Elution traces of **BP4**. 35°C in THF, elution at 1 mL/min.

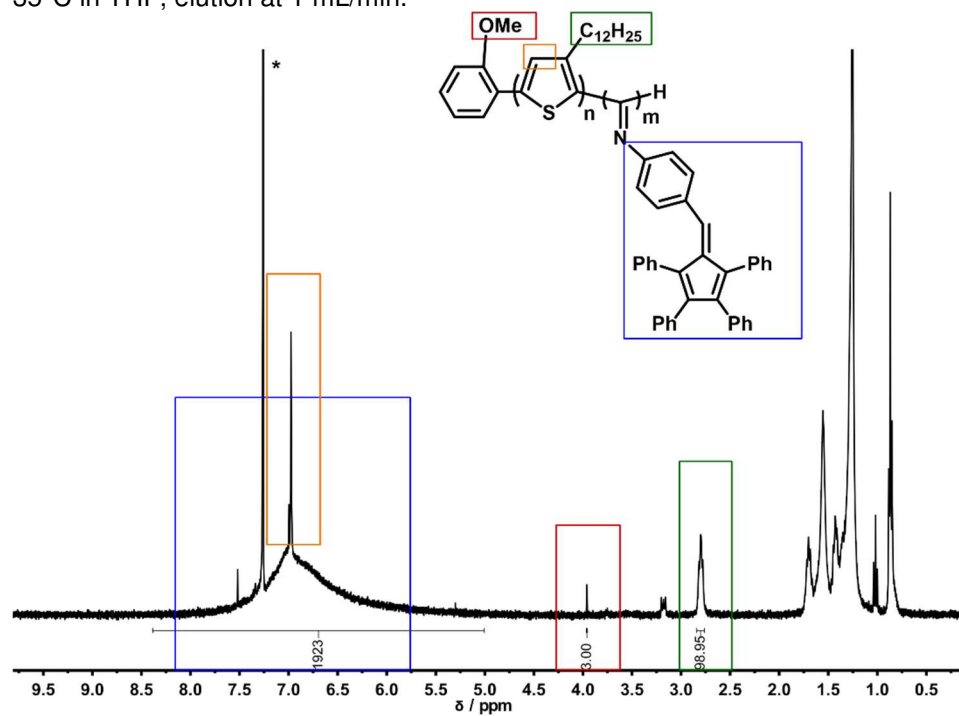


Figure S3. ¹H NMR spectrum of **P(3DT-b-IC2)** (feed 1:1). ¹³C-satellite signals of CHCl₃ also visible. Recorded in CDCl₃(*).

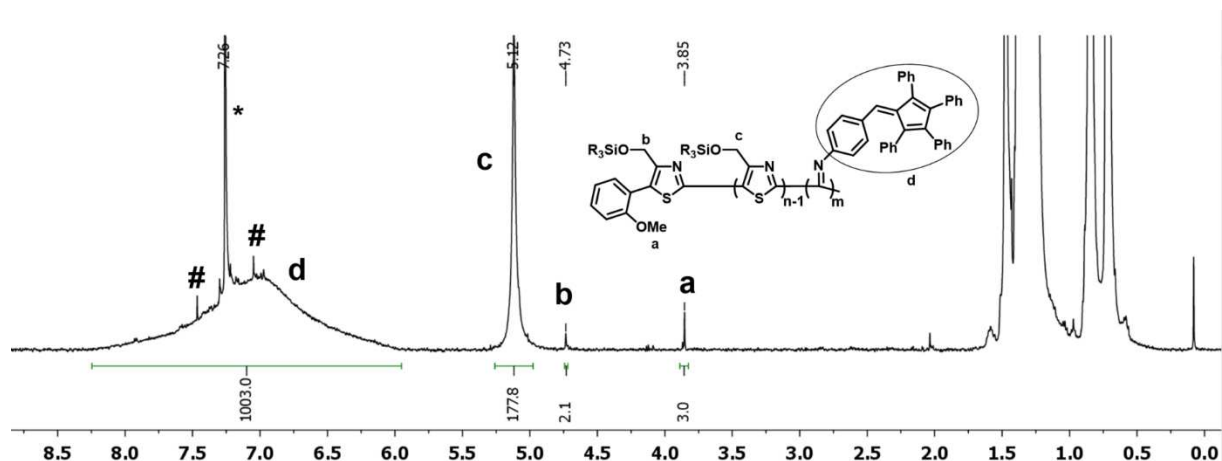


Figure S4. ^1H NMR spectrum of **P(TzTHX-b-IC2)** (**BP4**).
 # ^{13}C -satellite signals of CHCl_3 . Recorded in CDCl_3 (*).

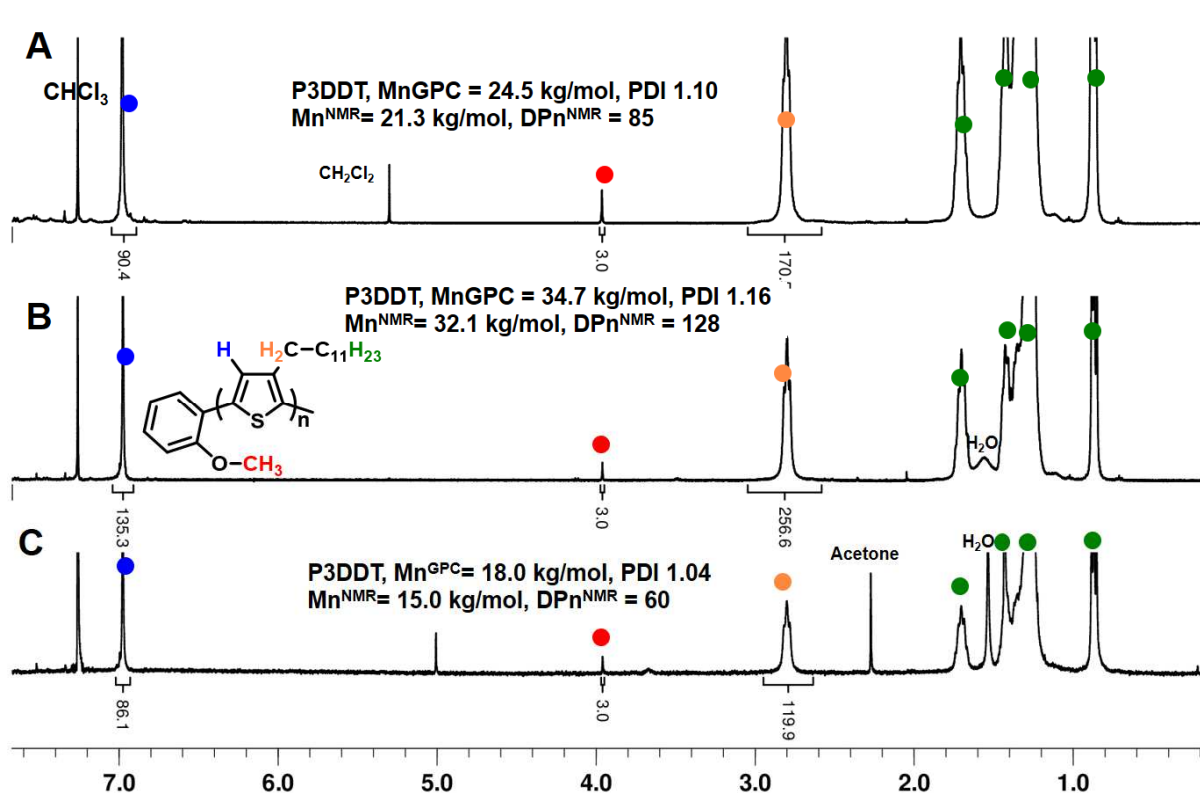


Figure S5. ^1H NMR spectra of anisyl-capped **P3DDT**.
 Spectra Recorded in CDCl_3 (*). The polymer were prepared analogously to the macroinitiators for **BP11-BP31**.

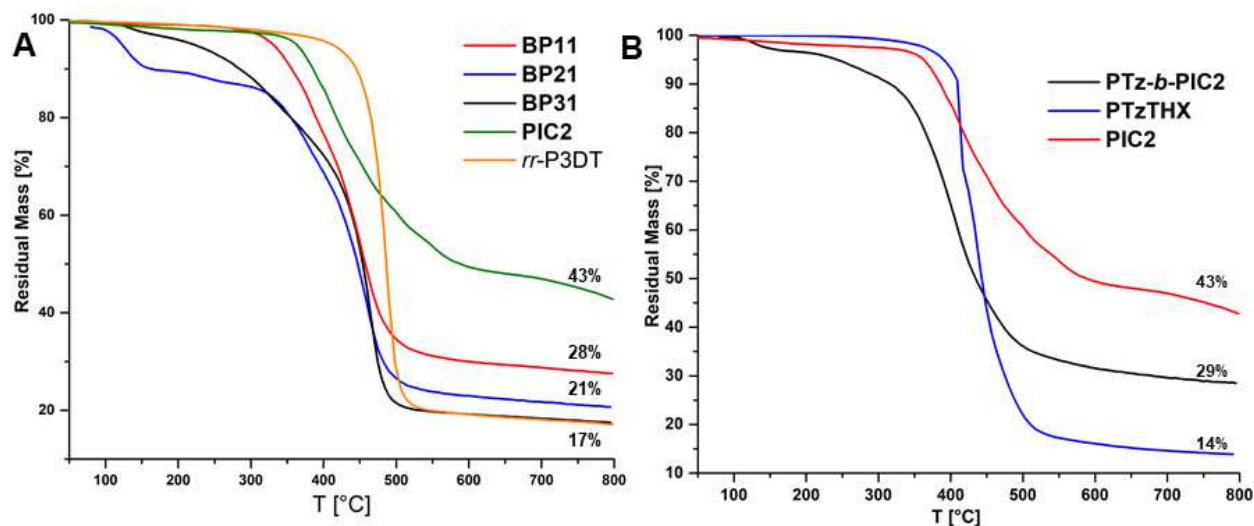


Figure S6. TGA thermograms of **BP11**, **BP21**, **BP31** (A) and **BP4** (B).

Data for *rr*-**P3DT** and **PIC2**, and **PTzTHX** included for reference. Heating rate 10°C per minute. The mass-loss of **BP21** between 100 and 150°C is attributed to evaporation of trapped solvent.

Comments: The relative proximity of the decomposition temperatures of **P3DT** and **PTzTHX**, to the one of **PIC2**, and the gradual degradation of **PIC2** above 400 °C, did not allow direct observation of sequential decomposition of the individual blocks. However, the residual masses of the BCPs at 800°C correlate with the relative content of **PIC2**, since **PIC2** leaves about 43 mass-% while **P3DT** and **PTzTHX** which leave just 17 and 14 mass-%, respectively (see also Table S1).

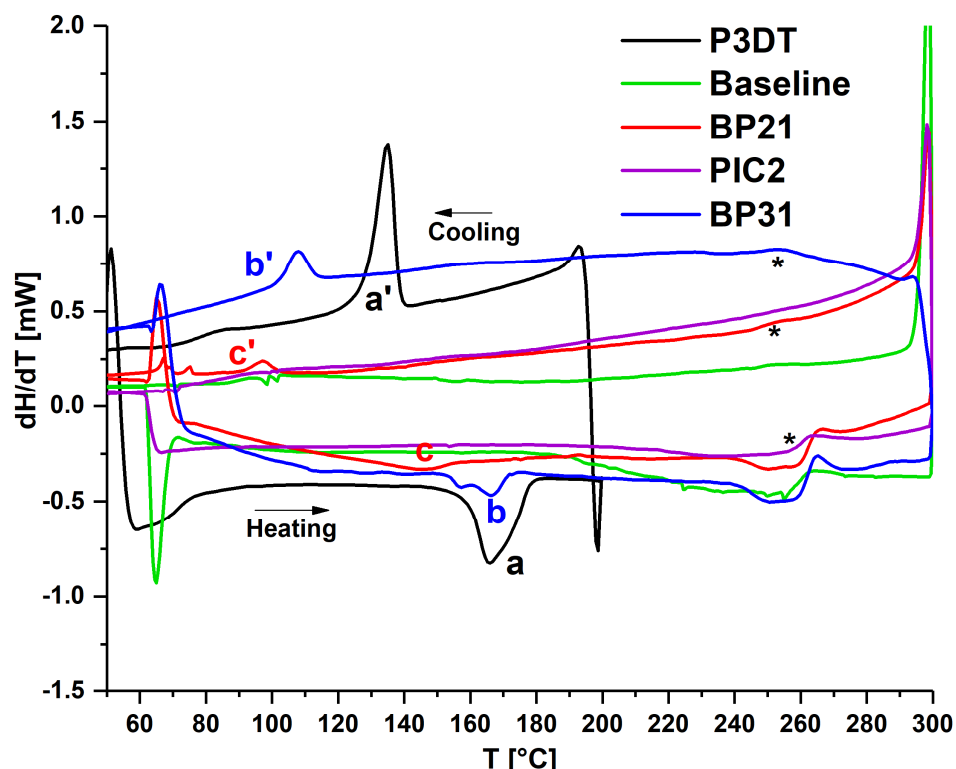


Figure S7. DSC thermograms of homo- and block-copolymers.

Heating rate 20°C per minute. * The artefact signal at 250-270 °C also present in the background scan. **PIC2** and **BP11** (not depicted) do not melt prior to decomposition. The melting points observed from **P3DT** agree with values from literature.¹⁰

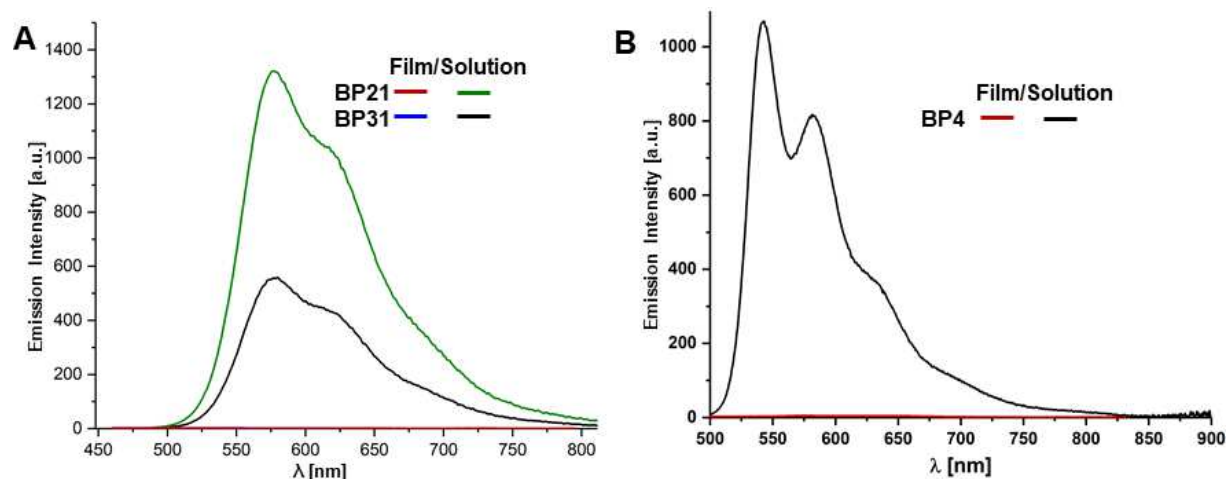


Figure S8. Fluorescence spectra of BCPs in solution vs. in the solid state. A) **BP31** and **BP21**, B) **BP4**. All solution spectra recorded in DCM.

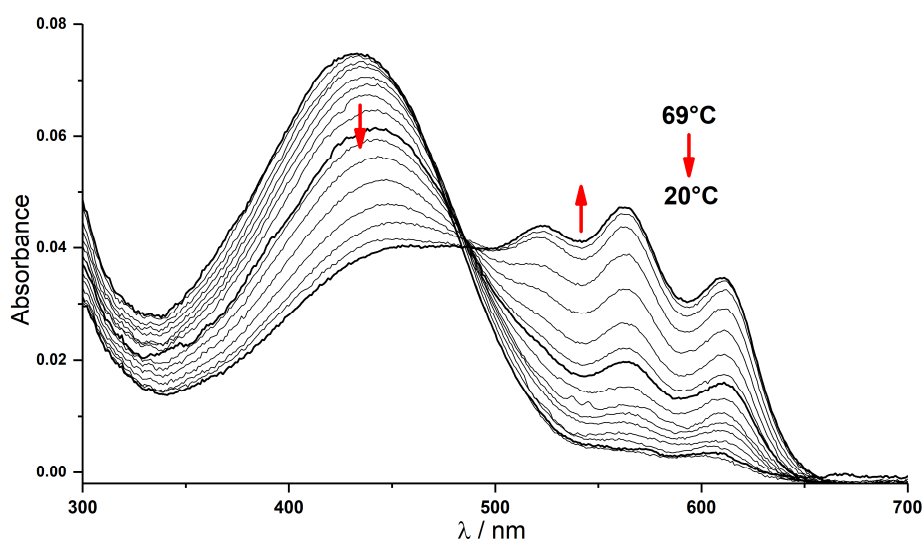


Figure S9. Aggregation of a **P3DT** in hot hexane monitored by UV-vis absorption

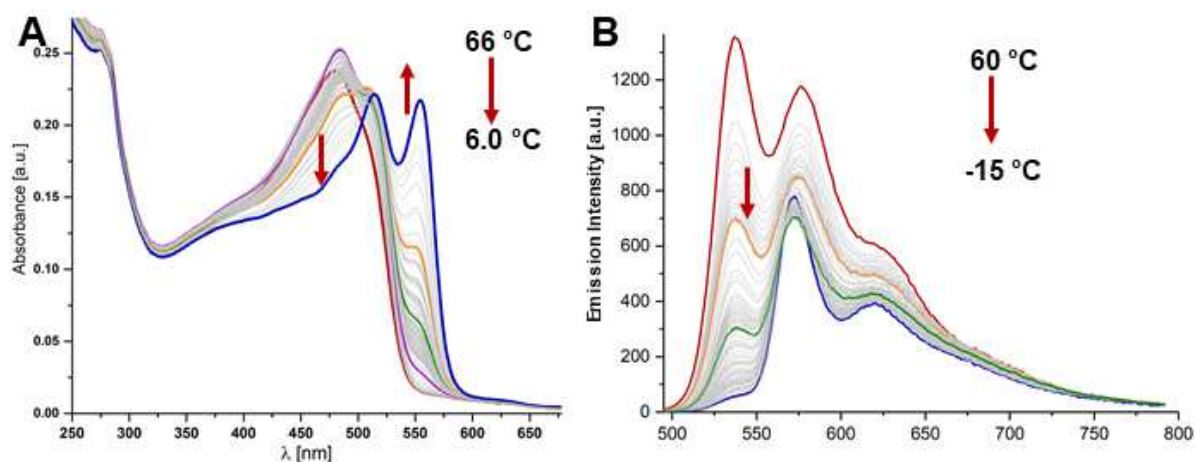


Figure S10. **BP4** in n-heptane solution monitored by UV-vis absorption and fluorescence spectroscopy.

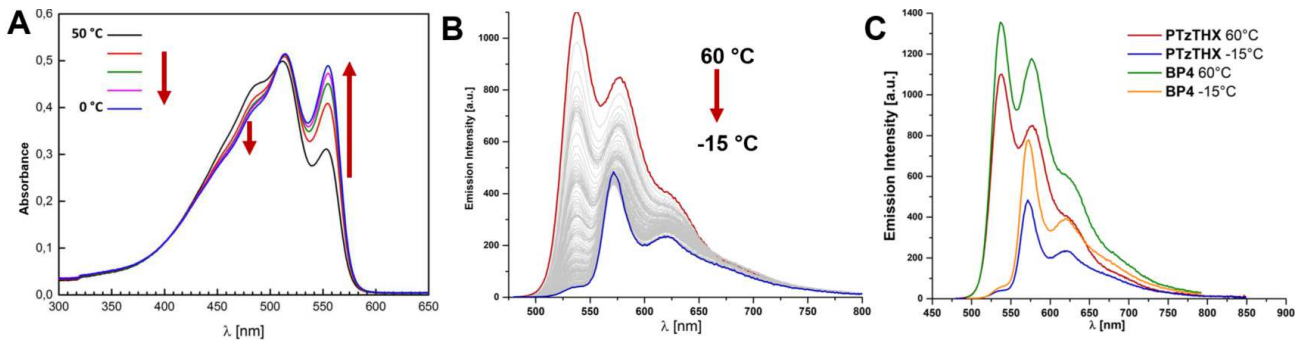


Figure S11. Temperature dependent UV-vis-data of **PTzTHX** in hexane solution. A) Absorption spectra. B) Fluorescence spectra. C) Comparison of fluorescence of **BP4** and **PTzTHX** in solution.

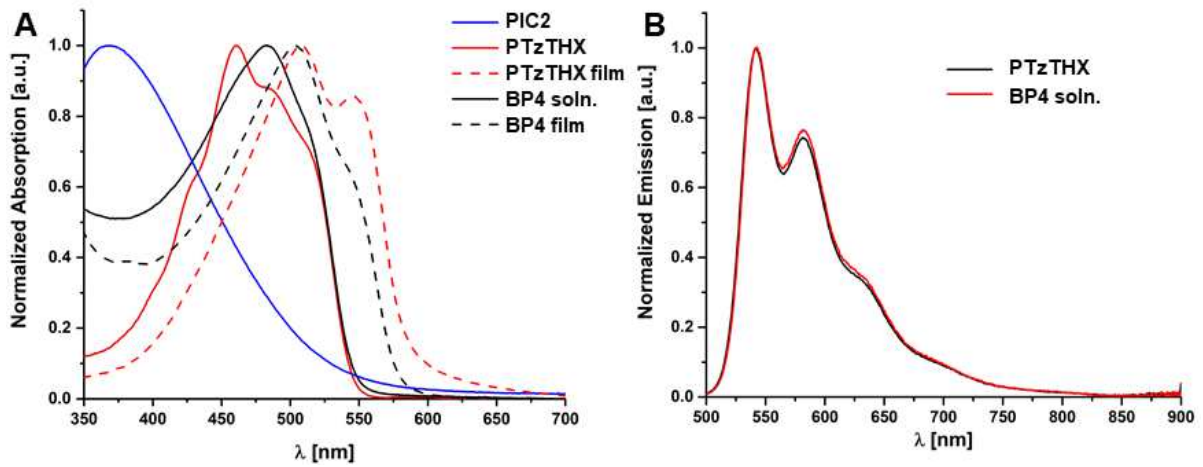


Figure S12. A) Absorption spectra **BP4** in DCM solution and of thin films, B) and emission spectrum recorded in DCM solution. Spectra for **PIC2** and **PTzTHX** included for reference.

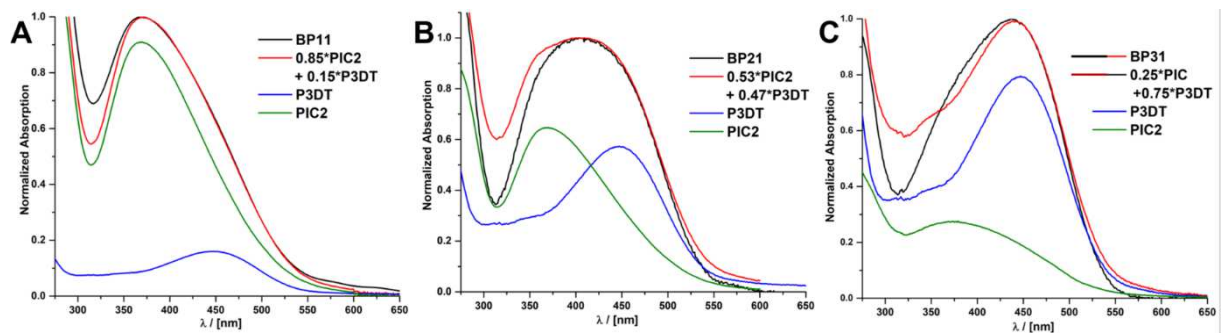


Figure S13. UV-vis spectra of BPCs reproduced by overlay of homo polymer spectra.

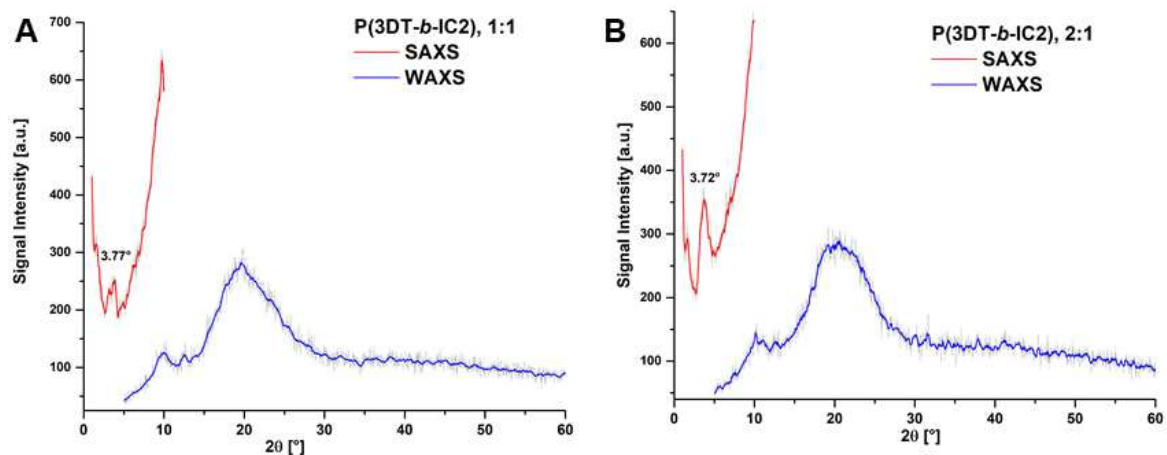


Figure S14. SAXS and WAXS refractograms of aggregated **BP11** (A) and **BP21** (B).

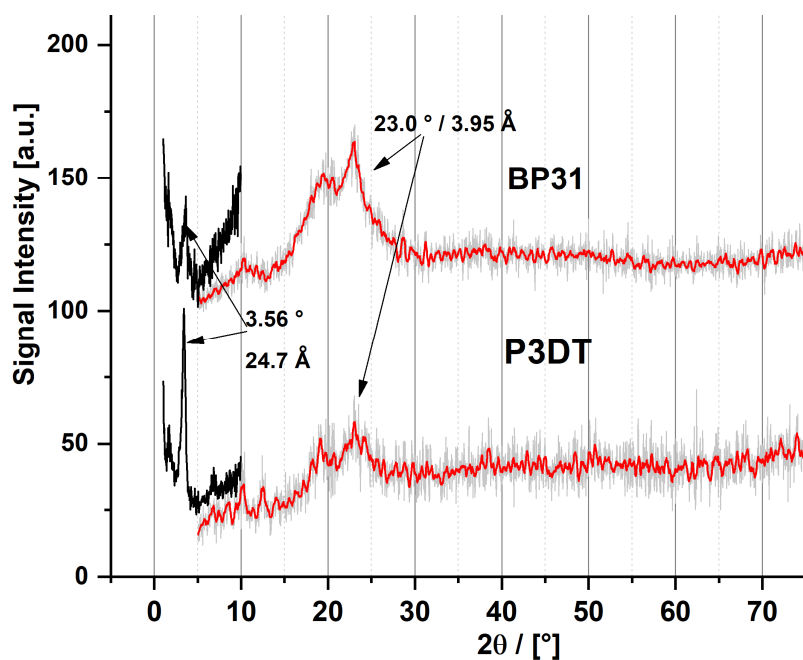


Figure S15. SAXS (black) and WAXS (red/gray) refractograms of **BP31** and a reference sample of **P3DT**.

Bulk samples retrieved after DSC measurements. Grey: experimental data, red: smoothed fit.

4. Electron Microscopy Data

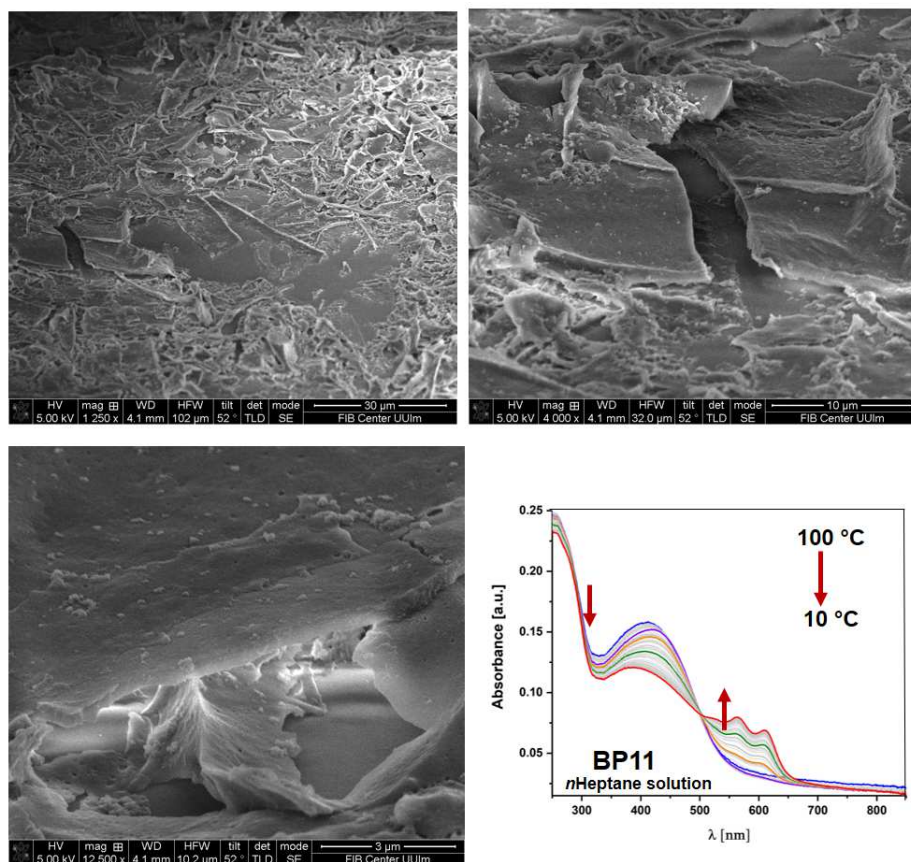


Figure S16. Scanning electron micrographs of aggregated BP11.

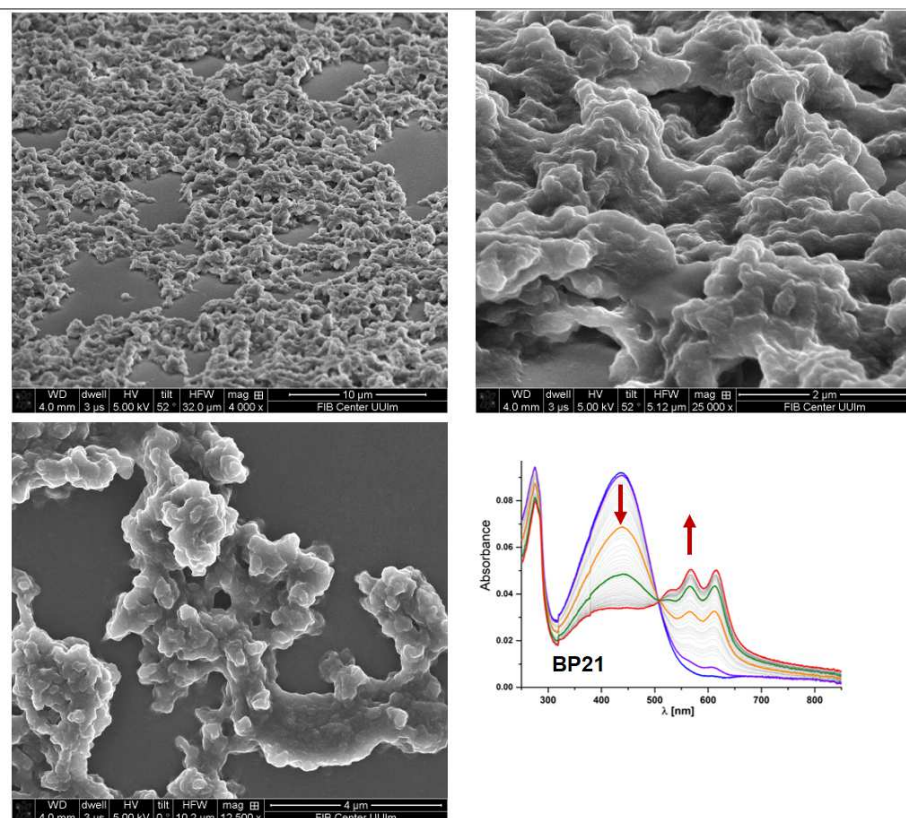


Figure S17. Scanning Electron Micrographs of aggregated BP21.

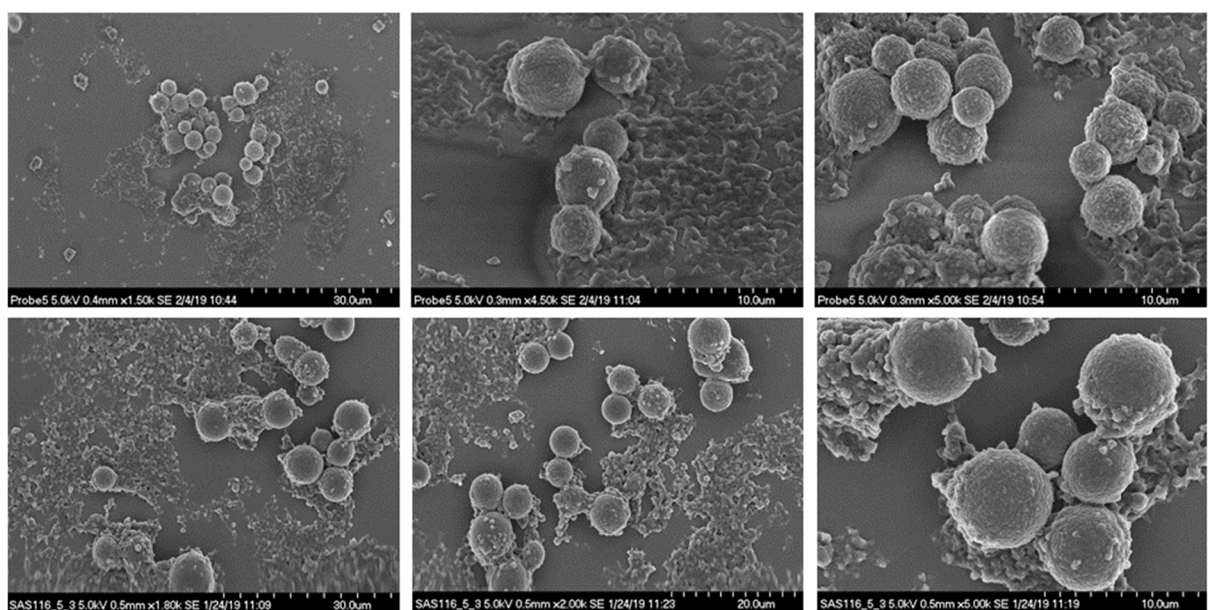


Figure S18. Scanning Electron Micrographs of aggregated **BP31** after fast cooling.

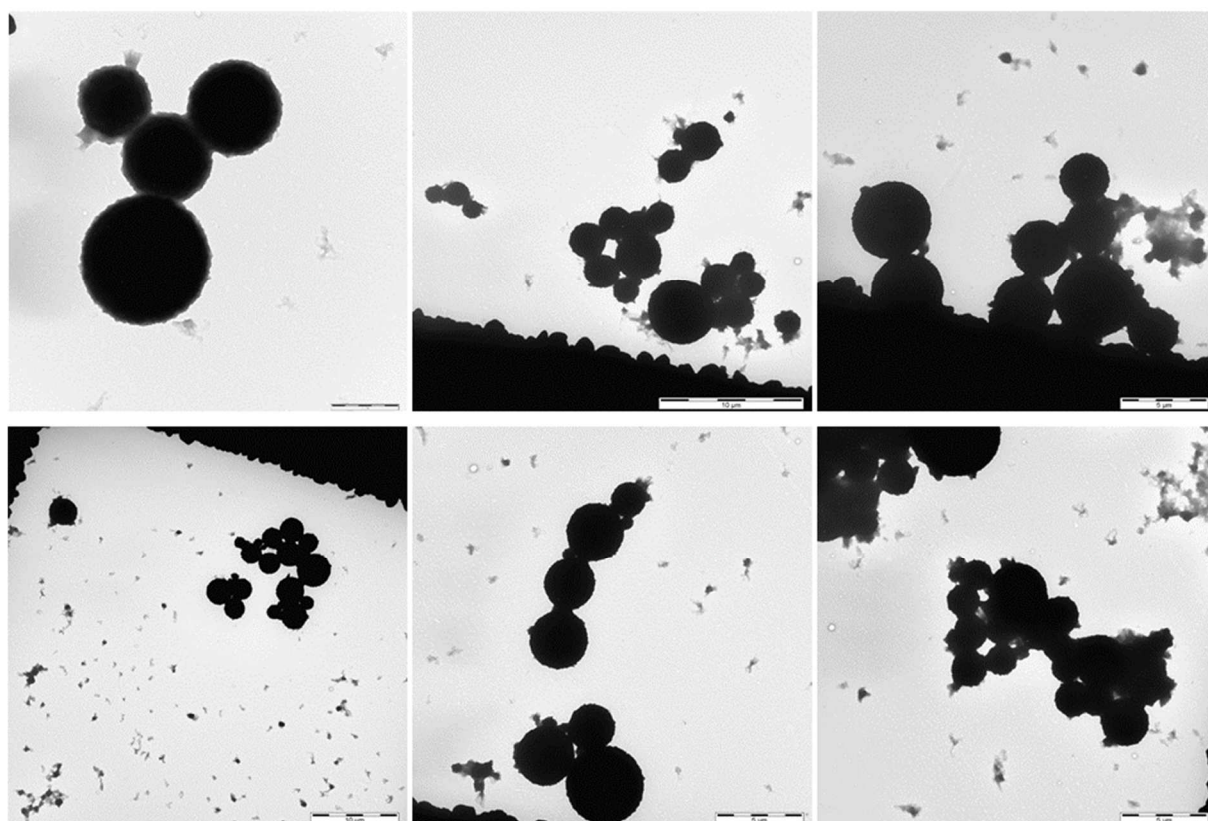


Figure S19. Transmission Electron Micrographs of aggregated **BP31** after fast cooling.

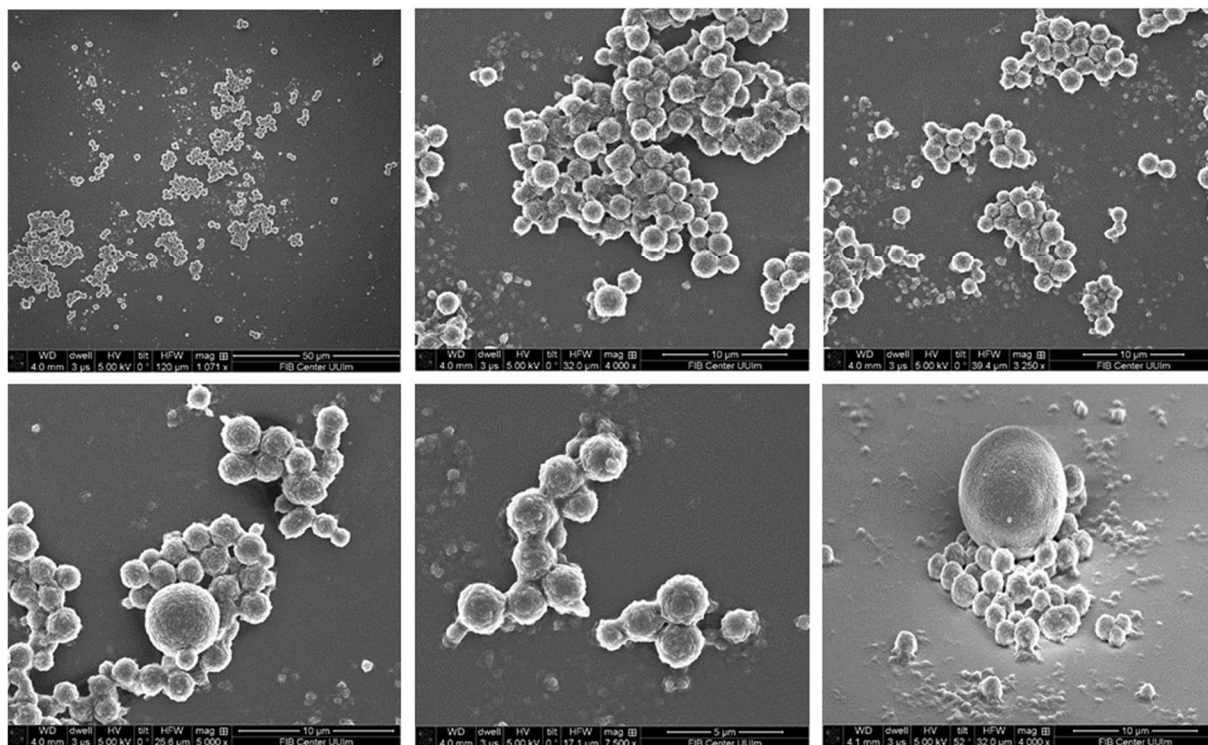


Figure S20. Scanning Electron Micrographs of aggregated **BP31** after slow cooling.

5. Electrical characterization and devices

5.1. Test in block-copolymer solar cells

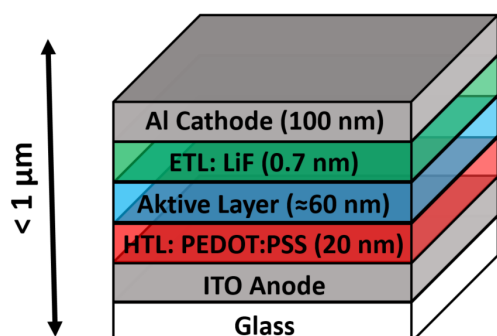


Figure S21. Device architecture used for block-copolymer solar cell.

ETL: Electron transport layer. HTL: hole transport layer, PEDOT:PSS: Poly(3,4-ethylenedioxythiophene) polystyrene sulfonate. ITO: Indium Tin Oxide.

Device fabrication: PEDOT:PSS (Clevios P, VP.AI 4083 Lösung von Heraeus) was doctor-bladed onto pre-cleaned, patterned indium tin oxide (ITO) substrates from Naranjo Substrates (15 cm²) at 50 °C upon 30–40 nm thick layers were obtained. The active layer solution of **BP11** (total concentration of 15 mg mL⁻¹, stirred at 80 °C for >1 h) was deposited by doctor-blading from chloroform at 80 °C. The cells were then annealed under chloroform vapor at 40°C for 1 min. Thin layers of LiF (0.7 nm) and Al (100 nm) were then deposited by high-vacuum evaporation at pressures <5 × 10⁻⁶ mbar (Nano 36, Kurt J. Lesker Co.). The photoactive areas of the cells were 0.09 and 0.16 cm². Finalized devices were evaluated using an Oriel Instruments solar simulator (class AAA, AM 1.5G, 100 mW cm⁻²) and a Keithley 2400 source meter. The EQE was measured under monochromatic light from a 300 W Xenon lamp in combination with a monochromator (Oriel, Cornerstone 260), modulated with a mechanical chopper. The response was recorded as the voltage over 220 resistance, using a lock-in amplifier (Merlin 70104). A calibrated Si cell was used as a reference (Newport 70356_70316NS).

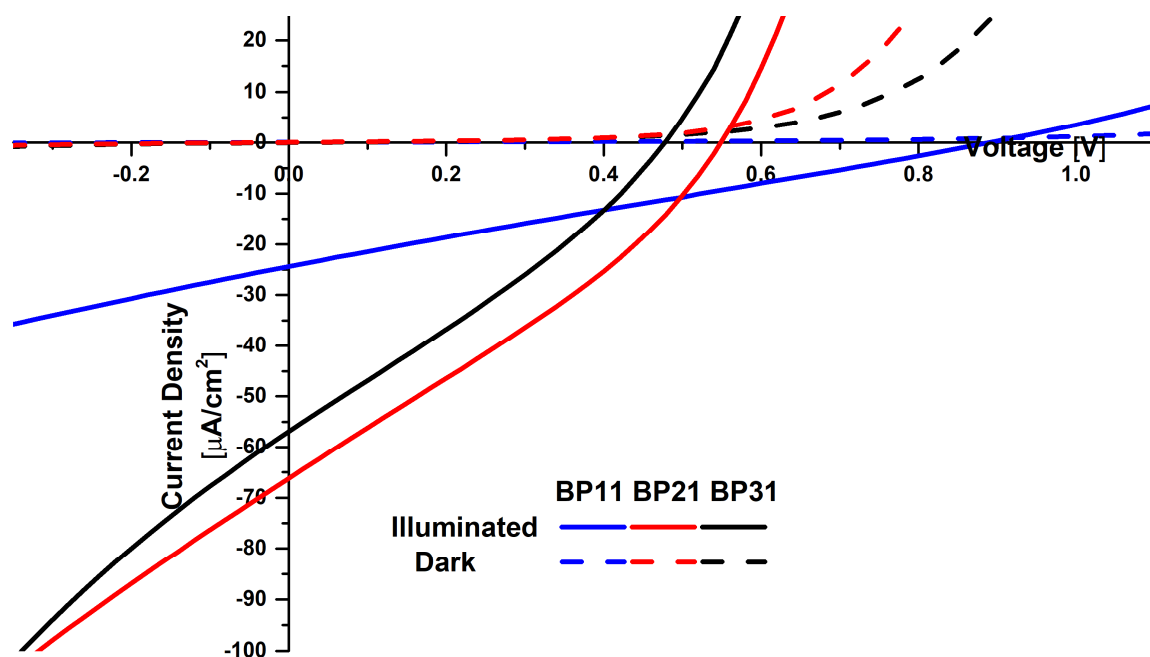


Figure S22. Current-Voltage curve for OSC-devices from **BP11**, **BP21**, and **BP31**.

Table S3. Solar cells performance of **BP11**, **BP21**, and **BP31**.

Entry	Polymer	Conditions	V _{oc} [V]	J _{sc} [μ A/cm ²]	FF	PCE [%]
1	BP11	AC	0.87	17.4	0.26	0.004
2		SVA	0.89	24.4	0.25	0.005
3	BP21	AC	0.65	38.7	0.25	0.006
4		TA	0.55	66.2	0.30	0.011
5	BP31	AC	0.45	45.6	0.30	0.006
6		SVA	0.48	56.9	0.29	0.008

AK: as cast from CHCl₃; TA: thermal annealing at 200 °C, SVA: solvent vapor annealing with CHCl₃

5.2. Electrical characterization of PIC1 – PIC3

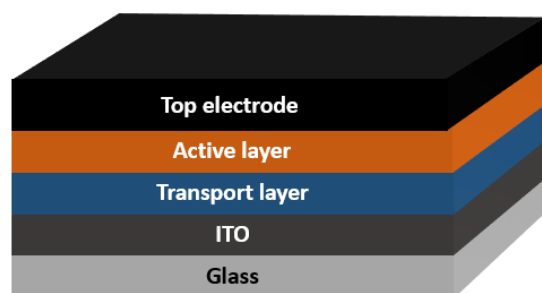


Figure S23. Device architectures used for mobility measurements.

Preparation of single carrier devices: Hole only diodes were fabricated with the structure: ITO/PEDOT:PSS/Polymer layer/MoO₃/Ag and electron only diodes were prepared with the structure: ITO/PFN-P1/Polymer layer/Ca/Al.

ITO patterned glass substrate was subsequently cleaned using acetone, isopropanol and MiliQ water in ultrasonic bath for 15 mins each, followed by UV-ozone treatment for another 15 mins.

For the hole only diode, PEDOT: PSS was dissolved in isopropanol with volume ratio 1:1. PEDOT:PSS solution was first filtered using a 0.45 μ m PVDF filter and there after spin coated onto the cleaned substrate at 3500 rpm for 30 s and then thermally annealed at 120^o C for 15 mins on a hot plate under ambient condition and transferred into the glove box for further processing. All the following procedures were done in nitrogen atmosphere.

For the electron only device, PFN-P1 was dissolved in methanol in the presence of a small amount of acetic acid (2 μ l/ml) with a concentration of 2 mg/ml and was left stirring overnight at room temperature. The PFN-P1 solution was filtered using a 0.2 μ m PTFE filter and spin-coated on top of cleaned ITO substrate at 3500 rpm for 30 sec.

PIC1, **PIC2**, or **PIC3** were dissolved in Chloroform with a concentration of 5mg/ml, and the solutions was left stirring overnight at 60^oC under nitrogen atmosphere. The polymer layer was spin-coated in two steps; first at 600 rpm for 30 sec and then at 1000 rpm for 10 sec to gain a smooth film.

Finally, a 10 nm of MoO₃ and 100 nm of Ag were thermally evaporated onto the polymer layer for hole only diode and a 20 nm of Ca and 100 nm of Al were thermally evaporated onto the polymer layer for electron only diode.

Electrical characterization of single carrier diodes: Electrical measurements were performed in the dark, inside a nitrogen filled airtight electrical holder. We performed current-voltage measurements on the single carrier diodes using a Keithley 2400 source meter controlled by a LabView program by scanning the voltage from -1V to +1 V.

The carrier mobility was extracted from the JV curves using Space Charge Limited Current (SCLC) theory. At low voltages, the current varies linearly with the applied voltage (Ohmic regime). At higher voltages, the current varies quadratically (SCLC regime). The carrier mobility μ is extracted from the JV curve at higher voltages by applying Child's law

$$J = \frac{9}{8} \epsilon \mu \frac{V^2}{d^3}$$

Where ϵ is the dielectric constant of the polymer (assumed to be 3) and d is the thickness of the polymer film.

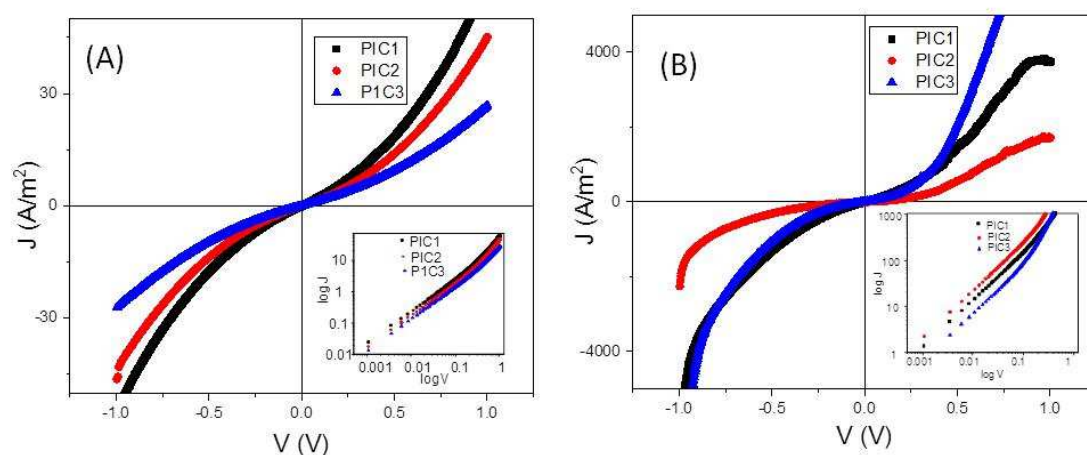


Figure S24. Current density versus Voltage (JV) curves of three exemplary single carrier devices, the inset image shows corresponding log J versus log V fitted curve used for the calculation of mobility (A) Hole-only diode behavior and (B) Electron-only diode behavior.

Table S4. Summary of mobility measurements for **PIC1**, **PIC2**, and **PIC3**.

Polymer	Electron mobility (cm ² /Vs)	Hole Mobility (cm ² /Vs)
PIC1	4.0*10 ⁻⁵ ±1.6	3.4*10 ⁻⁵ ±2.3
PIC2	1.04*10 ⁻² ±2.5	1.13*10 ⁻⁴ ±1.4
PIC3	4.0*10 ⁻⁴ ±2.8	2.1*10 ⁻⁵ ±1.56

6. References

- [1] a) S. Schraff, Y. Sun, F. Pammer, „Fulvenyl-functionalized Polyisocyanides – Cross-conjugated Electrochromic Polymers With Variable Optical and Electrochemical Properties”, *Macromolecules* **2018**, 51, 5323-5335; b) S. Schraff, Y. Sun, F. Pammer, „Correction to Fulvenyl-functionalized Polyisocyanides – Cross-conjugated Electrochromic Polymers With Variable Optical and Electrochemical Properties””, *Macromolecules* **2018**, 51, 18, 7417-7418.
- [2] a) A. Yokoyama, R. Miyakoshi, T. Yokozawa, *Macromolecules* **2004**, 37, 1169; b) H. A. Bronstein, C. K. Luscombe, *J. Am. Chem. Soc.* **2009**, 131, 12894; c) P. Kumari, K. Khawas, S. Hazra, B. K. Kuila, *J. Polym. Sci. Part A: Polym. Chem.* 2016, 54, 1785–1794.
- [3] J. Jäger, N. Tchamba Yimga, M. Urdanpilleta, E. von Hauff, F. Pammer, Towards n-Type Analogues to Poly(3-alkylthiophene)s: Influence of Side-chain Variation on Bulk-morphology and Electron Transport Characteristics of Head-to-tail Regioregular Poly(4-alkylthiazole)s, *J. Mater Chem. C* **2016**, 4, 2587-2597.
- [4] F. Pammer, J. Jäger, B. Rudolf, Y. Sun, Soluble Head-to-Tail Regioregular Polythiazoles: Preparation, Properties and Evidence for Chain-Growth Behavior in the Synthesis via Kumada-Coupling Polycondensation, *Macromolecules* **2014**, 47, 5904-5912.
- [5] W. L. F. Armarego, D. D. Perrin, Purification of Laboratory Chemicals, 4th Ed. Butterworth-Heinemann, Oxford, **1997**.
- [6] G. R. Fulmer, A. J. M. Miller, N. H. Sherden, H. E. Gottlieb, A. Nudelman, B. M. Stoltz, J. E. Bercaw, K. I. Goldberg, NMR Chemical Shifts of Trace Impurities: Common Laboratory Solvents, Organics, and Gases in Deuterated Solvents Relevant to the Organometallic Chemist. *Organometallics* **2010**, 29, 2176-2179.
- [7] P. Walther, C. Schmid, M. Sailer and K. Höhn “Is the scanning mode the future of electron microscopy in cell biology?” in *Scanning Electron Microscopy for the Life Sciences*, Edt. H. Schatten, Cambridge University Press, New York, **2012**, 71.
- [8] S. Schraff, Y. Sun, F. Pammer, Fulvenyl-functionalized Polyisocyanides – Cross-conjugated Electrochromic Polymers With Variable Optical and Electrochemical Properties, *Macromolecules* **2018**, 51, 5323-5335.
- [9] R. D. McCullough, R. D. Lowe, M. Jayaraman, D. L. Anderson. Design, synthesis and control of conducting polymer architectures: structurally homogeneous poly(3-alkylthiophene)s. *J. Org. Chem.* **1993**, 58, 904–912.
- [10] V. Causin, C. Marega, and A. Marigo Crystallization and Melting Behavior of Poly(3-butylthiophene), Poly(3-octylthiophene), and Poly(3-dodecylthiophene). *Macromolecules* **2005**, 38, 409 - 415